# DYNAMICS OF THE ANTARCTIC ICE CAP
## Part II : Sensitivity experiments with a numerical ice sheet model with full thermo-mechanical coupling

**Philippe HUYBRECHTS**

Vrije Universiteit Brussel
Geografisch Instituut
Pleinlaan 2 - 1050 Brussel
Belgium

---

*Proceedings of the Belgian National Colloquium on Antarctic Research*
*Brussels, October 20, 1987*
*Prime Minister's Services - Science Policy Office*

**Key words:** ice sheet, numerical modelling, thermo-mechanical coupling, Vostok ice core

**Abstract:** *An efficient numerical ice sheet model, including time dependence and full thermo-mechanical coupling, has been developed to investigate the thermal regime and overall configuration of a polar ice sheet with respect to changing environmental conditions.*

*From basic sensitivity experiments, in which a schematic East-Antarctic Ice Sheet is forced with a typical glacial-interglacial climatic shift, it is found that (i):the mutual interaction of temperature and deformation has a stabilizing effect on its steady state configuration and (ii) in the transient mode, this climatic transition initially leads to increased ice thickness due to enhanced accumulation, whereafter this trend is reversed due to a warmer base. Time scales for this reversal are of the order of $10^3$ years in marginal zones and of $10^4$ years in interior parts.*

*Time-dependent modelling of the Vostok flowline, indicates that the Vostok Station area has risen about 95 m since the beginning of the present interglacial due to thermo-mechanical effects, which is of particular interest in interpreting the palaeoclimatic signal of the obtained ice core there.*

## 1.Introduction

In polar ice sheets, ice flow and its thermodynamics are strongly related: temperature determines to a large extent the viscosity of ice so that for a 10 K temperature change, strain rates, for a given stress, change by an order of magnitude, thereby constituting a major factor in controlling the flow characteristics and shape of large polar ice sheets.

Physically, the interaction of temperature and flow comprises a positive feedback mechanism with regard to (sudden) global climatic changes, so that, in principle, creep instability may occur: the increasing ice temperature - increasing strain rate - increasing dissipation feedback-loop, may, under suitable circumstances, lead to a runaway temperature increase, resulting in extensive basal melting, ultimately bringing a continental ice sheet in the surging mode. The potential importance of creep instability in destabilizing the East Antarctic Ice Sheet has been stressed by several authors (Clarke et al. 1977; Schubert and Yuen, 1982; Yuen et al., 1986). However, as became clear in Huybrechts and Oerlemans (1988), the major objection against these analyses is that they are "local" : horizontal temperature advection and driving stress (ice sheet geometry) are not allowed to react to the changing temperature and velocity fields. The development of a creep instability in the aforementioned studies appears to be essentially the consequence of a basic shortcoming in model formulation, namely the neglect of horizontal heat advection, so that a basic damping mechanism is excluded.

From a climatological point of view, on the other hand, interpretation of temperature-depth profiles and isotopic composition of deep ice cores provides evidence of the history of climate, once we understand how ice sheets move and vary under changing conditions. To study the interaction of the physical processes involved, it is necessary to solve the equations governing ice-flow mechanics together with the thermodynamic equation in a fully time-dependent fashion. Historically, the first papers on the temperature distribution in ice sheets did not deal with the interaction of velocity and temperature, but were attempts to give a theoretical explanation for observed temperature profiles (e.g. Robin, 1955; Weertman, 1968; Philberth and Federer, 1971). In these calculations simple one-dimensional (vertical) steady-state models were involved. Due to the neglect of horizontal advection these models could only be applied in regions close to the ice divide. The moving-column model, based on a vertical model, but taking into account in a crude way the effect of horizontal advection, has subsequently been used to investigate two-dimensional (vertical plane) temperature distributions, see for example Budd et al. (1971) where this model is used extensively under steady-state conditions to assess the "Derived characteristics of the Antarctic Ice Sheet". This approach has been used widely by the Australian group since, also in more dynamic situations (e.g. Budd et al. ,1976; Young, 1981; Budd et al. , 1984). Critical to the applicability of the moving-column model is the vertical shear in the horizontal velocity as the assumption that the column remains vertical is not realistic far from an ice divide. Nevertheless, when ice motion is almost entirely by basal sliding, or when all velocity shear is concentrated in the lowest layers, the moving-column model works well. The model is also restricted to a stationary flow pattern since ice thickness is not a prognostic variable but instead used as input to derive the vertical mean horizontal velocity along a flowline.

To date, the most rigorous approach was taken by Jenssen (1977), who tried to solve the thermomechanical equations for "shallow ice flow" [for a more recent and more rigorous definition of shallow ice flow, see Hutter (1983)]. He introduced a scaled vertical coordinate, transformed the relevant continuity and thermodynamic equation (prognostic equations for ice thickness and temperature) and tried to solve the system numerically. In applying the scheme to the Greenland Ice Sheet, however, numerical instabilities occured, forcing the calculations to be interrupted after 1000 years of integration. In the last few years, Hutter et al. (1986) have presented numerical solutions for the steady-state two (vertical plane) dimensional case based on a treatment given by Morland (1984). However, in the paper by Hutter, it appears that numerical problems are still encountered, reducing the applicability of their solution to cases where the basal sliding velocity component has to be far larger than the movement due to internal deformation.

We recently developed a (three-dimensional), fully time-dependent ice sheet model (Huybrechts, 1986) with high resolution in the lower layers (i.e. where the shear concentrates). The inputs of this model are the mass-balance, temperature-dependent flow-law coefficients, the thermal parameters, surface temperature and the basal temperature gradient. We introduced a finite-difference scheme based upon the Alternating-Direction-Implicit method to solve the system numerically. This scheme appears to be stable, relatively efficient and seems to produce very realistic solutions.

Here, we report on some basic sensitivity experiments in which a schematic (East Antarctic) continental flowline is forced with 'glacial/interglacial' climatic conditions (accumulation and surface temperature) and its transient and steady state behaviour investigated. To conclude and assess the role of thermo-mechanical coupling in more realistic situations, the Vostok flowline is modelled. With relevance to the interpretation of the palaeoclimatic signal obtained at Vostok station

(Jouzel et al., 1987), special attention is paid here to a derivation of surface elevation changes following a glacial-interglacial climatic transition.

## 2. Model description

An elaborate description of the complete ice sheet model and the numerical procedures involved can be found in Huybrechts (1986). Here, only a brief outline will be presented. The numerical gridpoint model used in this paper describes ice flow along a flowline and computes the fully coupled velocity and temperature fields in a two-dimensional vertical plane, while accounting for any flow divergence or convergence in the continuity equation. Since integrating the thermodynamic equation in the computational stage on a grid fixed in space is rather inconvenient, as the upper and lower ice boundaries will generally not coincide with grid-points, a new vertical coordinate $\zeta$, scaled to the local ice thickness, has been introduced. Following Jenssen (1977) this stretched dimensionless vertical coordinate is defined by :

$$\zeta = \frac{H + h - z}{H} \tag{1}$$

such that $\zeta=0$ at the upper surface and $\zeta=1$ at the base for all values of x and t. In this definition H is ice thickness [m] and h bedrock elevation (zero at sea-level) in the usual Cartesian coordinate system (x,z,t), in which the x-axis is horizontal (x = 0 at the divide) and the z-axis is pointing upwards. The way in which equations are transformed to this non-orthogonal system $(x,\zeta,t)$, which will be used below, can be found in e.g. Haltiner (1971). In this approach, velocity and temperature fields are now computed at levels of constant $\zeta$ (the layer interfaces). For the experiments discussed in this paper, the vertical domain was subdivided into 10 layers concentrated towards the base with a lowermost gridspacing of $\Delta\zeta=0.02$, which proved to be sufficient to capture the essential characteristics of the model variables.

Ice deformation is assumed to result from shear strain, with the shear stress distribution in the model given by:

$$\tau(\zeta) = -\rho g H \zeta \frac{\partial (H + h)}{\partial x} \tag{2}$$

where the usual assumptions (sufficiently small bedrock and surface slopes, gridpoint spacings an order of magnitude greater than ice thickness) are used. In this expression g is acceleration of gravity and $\rho$ ice density [910 $kgm^{-3}$], taken to be constant.

Substituting this equation in a Glen-type flow law with exponent n=3 and integrating the resulting equation with respect to the vertical and using the above coordinate transformation, yields an expression for the horizontal velocity $u(\zeta)$:

$$u(\zeta) = 2(\rho g H)^3 H \left[\frac{\partial (H+h)}{\partial x}\right]^2 \frac{\partial (H+h)}{\partial x} \int_1^{\zeta} A(T^*)\, \zeta^3\, d\zeta + u(1) \qquad (3)$$

with basal boundary condition $u(1) = 0$.

The flow law coefficient $A(T^*)$ introduces the temperature dependence of ice deformation in the model. Apart from factors such as crystal fabric and impurity content, that might be equally important, laboratory experiments suggest that $A(T^*)$ obeys an Arrhenius relationship:

$$A(T^*) = m\,.\,a \exp\left[-\frac{Q}{R\,T^*}\right] \qquad (4)$$

In this expression a is specified below, R the universal gas constant [8.314 $Jmol^{-1}K^{-1}$], Q the activation energy for creep, and $T^*$ absolute temperature corrected for the dependence of the melting point on pressure ($T^* = T + 8.7\ 10^{-4}\ H\zeta$ , with T expressed in K). m is a tuning parameter and proved to be necesssary to slightly adjust the height-to-width ratio in some of the model runs. Its value is generally comprised between 1 and 10 and may be thought of as an implicit way to include the softening effect of crystal fabric and impurity content. Unless indicated otherwise in the text, the following values were chosen for a and Q: $T^* < 263.15$ K, $a = 1.14\ \ 10^{-5}\ Pa^{-3}year^{-1}$, $Q = 60$ $kJmol^{-1}$; $T^* \geq 263.15$ K, $a = 5.47\ \ 10^{10}\ Pa^{-3}year^{-1}$, $Q = 139$ $kJmol^{-1}$, so that $A(T^*)$ lies within the bounds as put forward by Paterson and Budd (1982).

Vertical motion [in m/year, negative downwards], as a result of accumulation and vertical strain, is calculated from the incompressibility condition, yielding:

$$w(\zeta) = \int_0^{\zeta} \left[ H \frac{\partial u}{\partial x}\Big|_{\zeta} + \frac{\partial u}{\partial \zeta} \left\{ \frac{\partial (H+h)}{\partial x} - \zeta \frac{\partial H}{\partial x} \right\} \right] d\zeta + w(0) \qquad (5)$$

with the kinematic boundary condition at the upper surface given by:

$$w(0) = \frac{\partial (H+h)}{\partial t} + u(0) \frac{\partial (H+h)}{\partial x} - M \qquad (6)$$

and M the local mass-balance [m/year], positive in the case of accumulation. Generally, the

calculated w at the ice-bedrock interface approached zero (if there is no sliding, the present case) within 0.01 m/year, revealing that the employed scheme conserves mass very well.
In order to adjust the flow-parameter A during the calculation, the temperature distribution within the ice sheet is found from the thermodynamic equation:

$$\frac{\partial T}{\partial t} = \frac{k}{\rho c_p H^2}\frac{\partial^2 T}{\partial \zeta^2} - u\frac{\partial T}{\partial x}\Big|_\zeta - \frac{1}{H}\frac{\partial T}{\partial \zeta}\left[\frac{\partial(H+h)}{\partial t} + u\frac{\partial(H+h)}{\partial x} - \zeta\left\{\frac{\partial H}{\partial t} + u\frac{\partial H}{\partial x}\right\} - w\right]$$
$$+ \frac{g}{c_p}\zeta\frac{\partial u}{\partial \zeta}\frac{\partial(H+h)}{\partial x} \qquad (7)$$

Here T is absolute temperature [K], t time [years], k thermal conductivity [6.62 $10^7$ $Jm^{-1}K^{-1}year^{-1}$] and $c_p$ specific heat capacity [2009 $Jkg^{-1}K^{-1}$]. In this equation heat transfer is considered to result from vertical diffusion (first term), horizontal advection (second term), vertical advection (included in the third term together with the various correction terms accounting for time-dependent layer geometry) and internal deformational heating due to horizontal shear strain rates. Boundary conditions follow from the mean annual air-temperature at the upper surface. At the base, neglecting heat conduction in the bedrock below, the geothermal heat flux is incorporated in the basal temperature gradient, taken to be 2K/100m. This corresponds to a heat flux of 4.2 $10^{-2}$ $Wm^{-2}$, considered as a value representative for East-Antarctica. Whenever the pressure melting point is reached, temperatures are set equal to that value. At the divide, all horizontal derivatives are zero.
In the model experiments discussed below, also the bedrock response has been taken into account, as the basal temperature distribution turns out to depend critically on total ice thickness. We considered a viscous asthenosphere, with lithosphere deflection following local hydrostatic equilibrium and an ice/mantle rock density ratio of 0.3:

$$\frac{\partial h}{\partial t} = D_a \frac{\partial^2}{\partial x^2}(h - h_0 + 0.3H) \qquad (8)$$

In this expression, $h_0$ is the undisturbed bedrock topography and $D_a$ [$10^8$ $m^2year^{-1}$] a diffusion coefficient. With a typical length scale of 1000 km, this equation leads to a relaxation time for bedrock adjustment of around 10000 years (Oerlemans and Van der Veen, 1984).
Finally, time-dependent evolution of ice thickness is described by:

$$\frac{\partial H}{\partial t} = -\frac{\partial}{\partial x}(HU) - \frac{1}{b}\frac{\partial b}{\partial x}HU + M \qquad (9)$$

with HU the vertically integrated mass flux per unit width given by:

$$HU = H \int_0^1 u(\zeta)\, d\zeta \tag{10}$$

and b(x) the width distribution along a flowline. In this paper, only 'half' an ice sheet is actually computed, with boundary conditions taken as zero thickness gradient (divide) and prescribed ice thickness at the edge (zero, unless indicated otherwise in the text).
In order to solve (9) numerically, this equation is written as a diffusion equation, with a 'vertically integrated' diffusion coefficient given by the scalar component of (10). We opted for a finite-difference approach, of the type implicit-in-time/central-in-space. A staggered grid in space was employed, in effect calculating mass-fluxes in between grid points with a mean diffusivity. Smoothing in this way turns out to keep the integration stable. The resulting finite-difference equations are usually quite readily solved with an explicit integration scheme. However, such a scheme has the important drawback that in order to preserve stability, time steps necessarily have to be taken small. Alternatively, a semi-implicit scheme, differing from a fully implicit method in that diffusivity is evaluated at the old time step, proved to perform very satisfactorily. Although not unconditionally stable, partly due to strong nonlinear coupling through the source terms, this scheme allows much larger time steps. The resulting tridiagonal linear systems are then easily solved by a Gaussian elimination method.
A comparable approach was taken to solve the thermodynamic equation. Here, the terms involving $\zeta$-derivatives were made implicit, leading once more to a set of tridiagonal equations to be solved at every grid point. However, a note concerning the horizontal advective terms is in order here, as replacing the derivatives by central differences turned out to generate oscillations in the solution. This problem is usually circumvented in diffusion-convection equations with a high Peclet number (i.e. a constant proportional to the ratio of advective velocity and diffusivity) by introducing an artificial horizontal diffusion process (e.g. Mitchell and Griffiths, 1980). We use an 'upwind' differencing scheme that can be shown to introduce an artificial horizontal diffusivity equal to $u.\Delta x/2$, with $\Delta x$ the grid spacing. Besides stabilizing the integration, this influences results only marginally, as in most cases the associated artificial heat transfer turns out to be an order of magnitude smaller than the horizontal heat advection term. In the experiments discussed here, spatial resolution was chosen to be 50 km. With this value, the flow part allows time steps from 50 up to 100 years, that were also used for the thermodynamic calculations.

## 3. Basic sensitivity versus environmental conditions

In order to investigate basic sensitivity of a polar ice sheet with respect to environmental conditions (accumulation and sea-level temperature) and to assess the role of the thermo-mechanical coupling, a series of (in first instance) steady state experiments was set up. For this purpose we considered a 'clean' flowline of uniform width, with a flat bedrock profile extending from the ice divide at x=0 to a fixed edge position at x=1500 km. First of all, a reference experiment was defined as follows: mean annual sea-level temperature and atmospheric lapse rate were set at 253 K and 12 K/1000 m respectively. Over the Antarctic Ice Sheet, the accumulation rate appears to be strongly correlated with surface temperature $T_S$ [K],(e.g. Robin and Johnsen, 1983), as the amount of precipitation is limited by the amount of water vapour that can be carried by the atmosphere at any temperature:

$$M = 2.5 \times 2^{\left\{\frac{T_S - 273.15}{10}\right\}} \qquad (11)$$

so that at a surface elevation of 3000 m, M=0.05 m/year, $T_S$=217 K and at sea-level M=0.625 m/year, respectively. With this parameterisation the mass-balance depends (in climatic change experiments)both on elevation and sea-level temperature.
Initially, computations started with zero ice thickness and bedrock elevation. Depending on the mass-balance, a steady state was usually established after 200000 to 300000 years of integration. With $\Delta x$ = 50 km, $\Delta t$ = 50 years and 10 layers in the vertical this required, including graphical output, about 300 CP seconds for every 100000 years and 130000 octal execution field length on a CDC-Cyber 175-750 computer. A realistic height-to-width ratio was obtained by setting m=10 in equation 4.

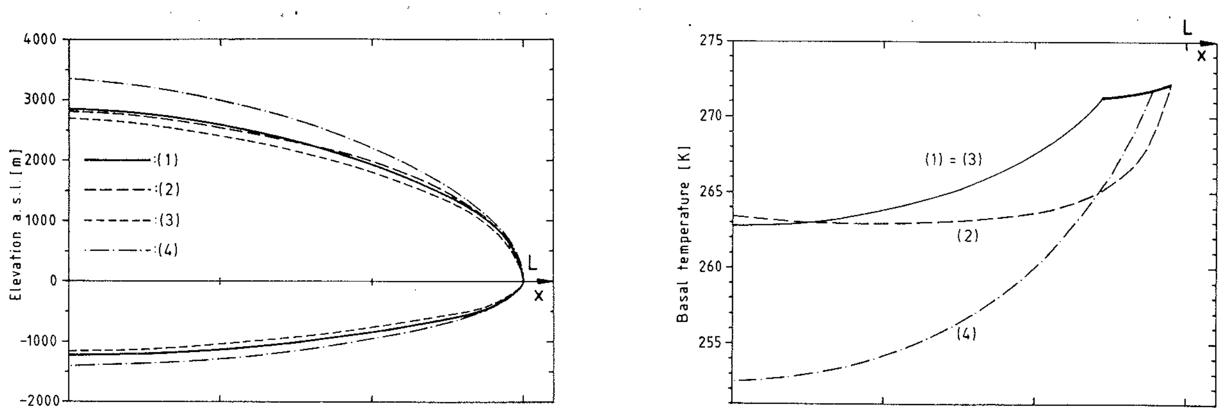


figure1: Steady state ice thickness (left) and basal temperature (right) distribution versus environmental conditions. (1): 'interglacial' reference run with sea-level temp. = 253 K; (2),(3),(4) are for sea-level temp. = 243 K, with (2): accumulation depending on surface temperature (corresponding shift in bed elevation is not shown) ; (3): fixed englacial temperature distribution; (4): fixed accumulation distribution with respect to (1). A thick line refers to pressure melting.

Basic sensitivity of the model to accumulation and/or sea-level temperature changes is displayed in fig.1. Keeping the accumulation distribution fixed with respect to the 253 K reference run (full line) and decreasing sea-level temperature only (point-dashed line), results, not surprisingly, in an increased ice thickness distribution, while the reverse is true for the basal temperatures. The sensitivities found here reflect the combined effect of many competing feedback mechanisms, such as the positive feedback of elevation changes on surface temperature, and the opposing effects of increased ice thickness leading to basal warming, together with the influence due to differences in deformational heat release (although relatively unimportant in this case). The short-dashed line in fig. 1 refers to a sensitivity experiment in which the temperature distribution of the ice sheet was held constant, so in effect showing the effects of changes in accumulation on ice thickness due to ice dynamics only. In this case there exists a negative feedback of accumulation on surface elevation: lower elevations tend to result in increased precipitation rates.

However, in the full-model run, where sea-level temperature, and, accordingly, accumulation rates vary, and full thermo-mechanical coupling is considered, colder conditions (long-dashed line) actually lead to slightly decreased ice thickness in central regions and slightly increased ice thickness in marginal zones, in spite of decreased dissipation and the rather important dependence of ice thickness on changes in surface temperature alone. As the concomitant change in basal temperature in the 'inner half' appears to be quite small, this means that in this particular situation, decreased advection of colder ice towards the basal shear layers associated with the 'glacial' accumulation rates, approximately compensates for the cooling effect of decreased surface temperature. So, generally speaking, the mutual coupling of temperature and velocity seems to have a stabilizing effect on the steady state configuration of a large polar ice sheet like East-Antarctica, submitted to different climatic environments within realistic ranges: the integrated effects of roughly doubling accumulation rates and raising sea-level temperature by 10 K (a typical glacial-interglacial climatic shift) on steady state ice thickness appear to be of similar magnitude, but of opposite sign.

Up to now only steady states were investigated. How these ice sheets actually evolve from one state to another at different locations is a different matter, if one realizes that the various terms in the heat equation all operate on different time-scales. Fig. 2 shows the evolution of ice thickness and basal temperature at 4 locations (labelled in increasing order outwards to the margin) following a linear 10000-year glacial-interglacial temperature rise of 10 K, starting from a steady state 243 K 'glacial' ice sheet (this is the state represented by the long-dashed line in fig.1). Basal temperatures (lower panel) initially increase with higher values downstream, later on counteracted by advection of cooler ice, resulting in a slight basal cooling. After that, temperature rises slightly again, related to the arrival of a strongly diffused 'warm wave', as a result of increased surface temperatures conducted towards the base. Note also that near to the divide (where there is hardly any dissipation) basal layers are actually cooling, as a result of increased vertical advection of cold ice.

The evolution of ice thickness (fig.2, upper panel) follows a somewhat opposite trend. Increased accumulation rates initially lead to increased ice thicknesses. This trend is then reversed as a result of enhanced shear strain due to a warmer base. Eventually, this 'lowering wave' travels upstream and reaches the divide in a much weakened form some 20000 years later. Following these results, it may thus very well be possible that at present, (mainly outer) parts of the Antarctic Ice Sheet are actually lowering as a delayed response on the increased accumulation rates associated with the last interglacial warming. Apparently, dependence of ice deformation on temperature adds a very long time scale to the system. Also, in these experiments no sign was found of runaway behaviour. The dissipation-strain rate feedback seems to be far too weak to give rise to massive basal melting. As demonstrated in Huybrechts and Oerlemans (1988), also the horizontal heat advection term plays a crucial role in damping any runaway temperature increase.

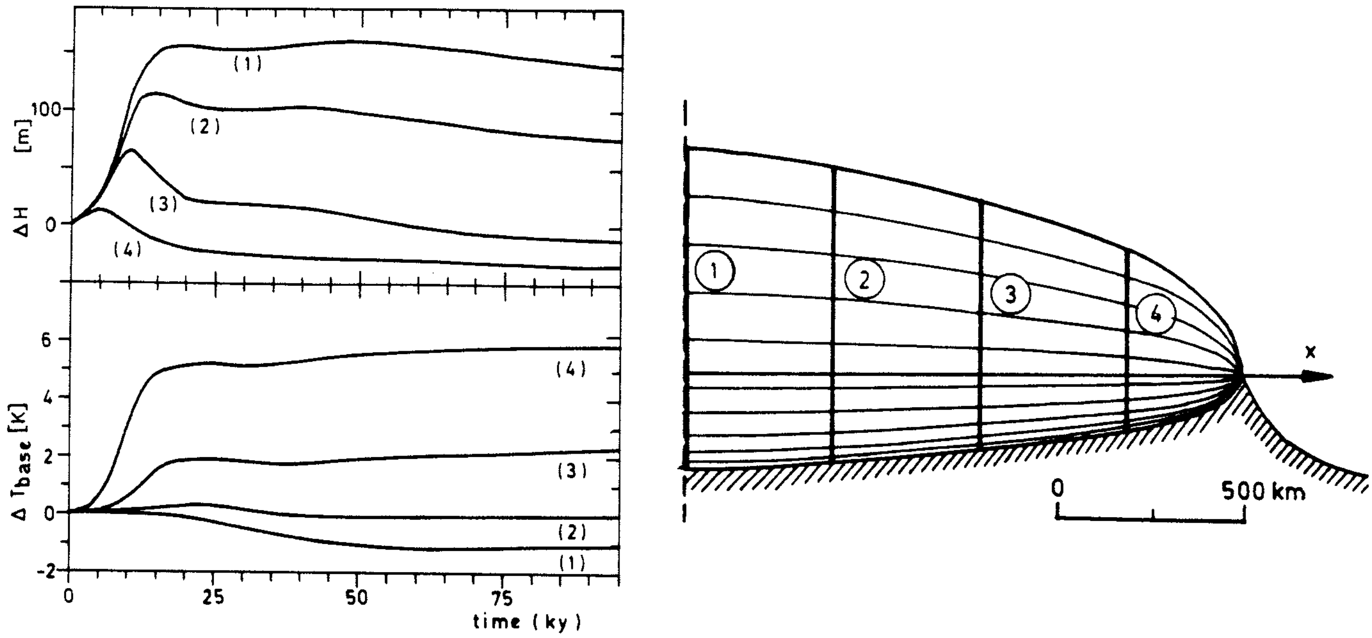


figure 2: Differences in ice thickness (upper panel) and basal temperature (lower panel) following a linear 10K glacial-interglacial climatic shift over 10.000 years starting at t=0. Locations in the ice sheet labelled (1) to (4) are shown to the right.

## 4. A calculation on the Vostok flowline.

To investigate implications of the thermo-mechanical coupling for the evolution of (a part of) the East Antarctic Ice Sheet with emphasis on the glacial-interglacial contrast, the Vostok flowline was modelled (fig.3). This flowline is of particular interest because local surface elevation changes in the Vostok station area also contribute in the isotope surface temperature signal recovered there (Jouzel et al., 1987), and hence, should be filtered out before a final assessment of these data can be made. Bedrock and surface elevation were digitized on a 50 km-grid along the flowline (of total length 1450 km), taken from the Antarctic glaciological and geophysical folio (Drewry, 1984). Present day accumulation rates (not shown) were taken from a preliminary map produced at SPRI, that also provided a tape with the original accumulation and surface temperature point measurements (Drewry, personal communication). Other parameters for the flowline include: present sea-level temperature = 248K ≈ -25 °C; surface temperature lapse rate = $-0.00875\ \mathrm{Km}^{-1}$; m = 7.
Bed elevation was assumed to be in isostatic equilibrium with present day ice thickness. Fig.3

shows the geometry of the modelled flowline, representing a steady state under present interglacial conditions. Although the experiments conducted so far clearly indicate that the Antarctic Ice Sheet is probably never in a steady state, the tuning parameter m could be chosen (independent on x) such that the modelled surface elevations approached measured surface elevations within 100 meters or less, which we feel proves the validity of the model equations. The Vostok flowline is debouching into the Ross Ice Shelf, where present-day ice thickness (800 m) is a boundary condition. As our present interest is focused towards thermo-mechanical response behaviour, changes in the length of flowlines due to sea-level changes or possible grounding line movement were isolated from the experiments. The corresponding steady state basal temperature distribution during present interglacial conditions is also shown in fig. 3 (lower panel, right). As a general tendency, basal temperatures tend to rise towards the edge (mainly a consequence of increased dissipation) and appear to be strongly controlled by local ice thickness due to the insulating effect of ice.

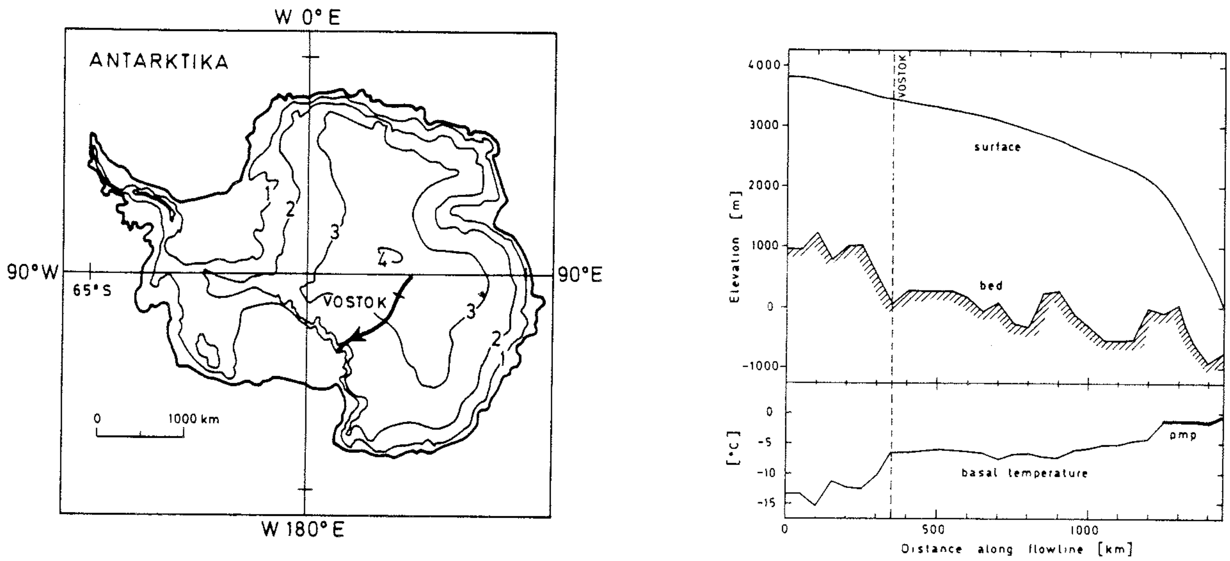


<u>figure 3:</u> Modelled steady state configuration (upper panel) and basal temperature distribution (lower panel) of the Vostok flowline under present interglacial conditions.

In a last experiment, the Vostok flowline was forced with a linear 10K glacial-interglacial sea-level temperature shift over 6000 years, starting from a steady glacial state 16000 years ago (fig.4, upper panel, right), as a general climatic trend deduced from Antarctic ice core data (Robin, 1983). Accumulation rates along the flowline were then calculated as described by Lorius <u>et al.</u> (1985). First, the temperature of formation of precipitation $T_f$ is assumed to be close to the temperature prevailing above the surface inversion layer, leading to (Jouzel and Merlivat, 1984):

$$T_f\,[\mathrm{K}] = 0.67\,T_s\,[\mathrm{K}] + 88.9 \qquad (12)$$

Then, accumulation rates were calculated from the product of its present value, times the ratio of the derivatives of the saturation vapour pressure over a plane surface of ice (e.g. Kraus, 1972), with respect to $T_f$ for the time of precipitation, and with respect to $T_f$ for present conditions.

$$M\,[T_f(t)] = M\,[T_f(\text{present})]\,.\,\exp\left\{ 22.47\left[\frac{T_0}{T_f(\text{present})} - \frac{T_0}{T_f(t)}\right]\right\} . \left\{\frac{T_f(\text{present})}{T_f(t)}\right\}^2 \quad (13)$$

For surface temperatures prevailing over central Antarctica, this glacial-interglacial temperature shift roughly halves present-day accumulation rates. $T_0$ = 273.16 K is the triple point of water.

Resulting shifts in surface elevation and basal temperature at present (time = 0) and after a final steady state has been established (taking up to 300000 years of integration) are displayed in fig.4. As shown before, the thermo-mechanical coupling adds a very long time scale to the system. As a consequence, a steady state description is quite inappropriate to deduce the present state of the ice sheet with respect to glacial conditions, as is immediately clear from fig.4. At present, surface elevations appear to have risen typically around 100 m in the central area, while the more coastal region appears to have thinned slightly under the influence of a basal temperature increase. This situation compares well with the response behaviour of other East Antarctic flowlines under similar conditions (Huybrechts and Oerlemans, 1988) and is also in agreement with the findings of Lorius et al. (1984), on the basis of total gas content in ice cores.

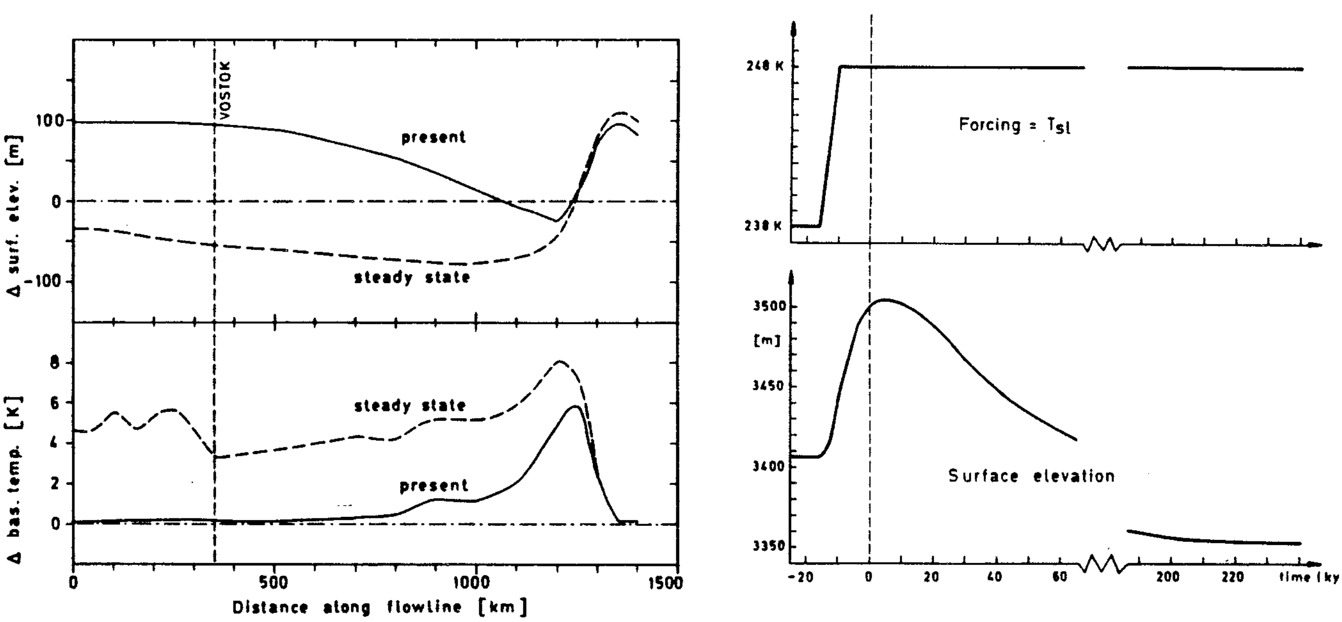


figure 4: Modelled evolution of the Vostok flowline, showing the forcing function (upper panel, right) and differences in surface elevation (upper panel, left) and basal temperature (lower panel, left) at present (time = 0) and after a steady state has been reached. The evolution of surface elevation at Vostok station is shown at the right (lower panel).

In the steady state, on the other hand, changes in surface elevation (amounting to a 0.7 fraction of total ice thickness) indicate a steeper margin and a smaller slope immediately upstream. This results from the warmer base and higher velocities in the outermost area and may also be due in part to a fixed outer boundary condition (where the surface elevation shift is zero, not shown on the graph). The concomitant rise in basal temperature remains below the applied sea-level forcing (10 K).

In central areas, due to the low velocities and the long time-scale connected with diffusion, basal temperatures have at present not shown any response yet and are still at the glacial level. Here again, steady state basal temperature shifts appear to be controlled by local ice thickness, in the sense that the thicker the ice, the more important becomes the cooling effect following increased vertical advection relative to warming due to vertical diffusive conduction effects (fig.4, lower left panel).

A point of particular interest here is Vostok station (fig.4, right), as elevation changes constitute a complicating factor in interpreting the palaeoclimatic signal of the obtained ice core there (Lorius et al., 1985). According to the calculations, the change in elevation since the beginning of the present interglacial 16000 years ago amounts at this moment to about +94 m. The model predicts the surface to rise another 6 m during the next 6000 years, whereafter, if climate were unaltered, it would be lowered by 150 m before setting down to a new steady state. Neglecting a (small) correction related to the origin of ice (deeper ice originated further upstream) and using a fixed atmospheric lapse rate (-0.00875 $Km^{-1}$), this calculation indicates that the inferred 16000BP-0BP climatic contrast in the core would be underestimated by about 0.8K due to elevation changes connected with the thermo-mechanical coupling.

## 5. Concluding remarks

In this study, the response of a continental polar ice sheet to changing climatic conditions was investigated using an efficient numerical model. This model differs mainly from previous models that it computes the mutually interactive temperature and velocity fields and that no a priori assumptions are made regarding their profiles or a steady state. As this model contains enough degrees of freedom and produces relevant boundary conditions, it serves as a 'core' towards the development of a general polar ice sheet model.

With emphasis on the glacial-interglacial climatic transition, our model calculations have shown that the thermo-mechanical coupling has a stabilizing effect on the steady state configuration of a schematic East-Antarctic Ice Sheet. In time-dependent experiments, the model shows a relatively fast response of ice thickness to increased accumulation rates, followed by a lowering trend due to warmer bases that travels slowly upstream. Time scales for this reversal are of the order of $10^3$ years in the margins and of $10^4$ years in central zones. Also, temperature-dependent creep behaviour of ice appears to add a long time scale to the system, indicating that the Antarctic Ice Sheet is probably never in a steady state.

Modelling the Vostok flowline, indicates that surface elevations near to the ice divide have risen around 100 m since the beginning of the present interglacial, while coastal areas may have thinned slightly. This means that the palaeoclimatic signal obtained at Vostok station is primarily of climatic origin. However, before a final assessment of level fluctuations at Vostok station can be made, the effects of, in particular, heat conduction in the bedrock below and changes in the horizontal model domain should also be looked at in more detail. Recent work by Ritz (1987) suggests that taking into account temperature conduction in the rock below the ice sheet roughly halves the basal temperature response (that would increase elevation shifts). On the other hand, as indicated by Alley and Whillans (1984), grounding-line retreat following a postglacial sea-level rise may have caused significant thinning of central East Antarctica since the Last Glacial Maximum. We intend to study these additional effects in the near future.

The strong dependence of basal temperatures and general climate sensitivity on geometry and topography necessitates the extension of this study to a fully three-dimensional calculation. With present-day supercomputers it is certainly possible to repeat the sensitivity experiments with a 100 km grid for the entire Antarctic Ice Sheet. Such a study is on the way.

## Acknowledgement

I thank Hans Oerlemans for his encouragement and very helpful discussions. Philippe Huybrechts is supported by the National Fund for Scientific Research (N.F.W.O.) and in part sponsored by the Belgian Ministry of Science Policy under contract ANTAR/04.

## References

Alley R B, Whillans I M (1984) Response of the East Antarctic Ice Sheet to sea-level rise. J.Geophys.Res. 89: 6487-6493

Budd W F, Jenssen D, Radok U (1971) Derived physical characteristics of the Antarctic Ice Sheet. ANARE Interim Report, Series A (IV) Glaciology, Publ. 120: 178 p. + maps

Budd W F, Young N, Austin C R (1976) Measured and computed temperature distributions in the Law Dome Ice Cap, Antarctica. J.Glaciology 16: 99-110

Budd W F, Jenssen D, Smith I N (1984) A three-dimensional time-dependent model of the West Antarctic Ice Sheet. Annals of Glaciology 5: 29-36.

Clarke G K, Nitsan U, Paterson W S B (1977) Strain heating and creep instability in glaciers and ice sheets. Rev. Geoph. Space Phys. 15: 235-247.

Drewry D J (1984) Antarctic glaciological and geophysical folio. Scott Polar Research Institute. Cambridge

Haltiner G J (1971) Numerical weather prediction. John Wiley. New York. 317 p.

Hutter K (1983) Theoretical Glaciology. D.Reidel. Dordrecht. 510 p.

Hutter K , Yakowitz S, Szidarovszky F (1986) A numerical study of plane ice-sheet flow. J. Glaciology 32:139-160.

Huybrechts Ph (1986) A three-dimensional time-dependent numerical ice sheet model for polar ice sheets: some basic testing with a stable and efficient finite-difference scheme. Intern rapport VUB:44p.

Huybrechts Ph, Oerlemans J (1988) Evolution of the East Antarctic Ice Sheet: a numerical study on thermo-mechanical response patterns with changing climate. Annals of Glaciology 11:in press.

Jenssen D (1977) A three-dimensional polar ice sheet model. J. Glaciology 18: 373-390.

Jouzel J, Merlivat L (1984) Deuterium and Oxygen 18 in Precipitation: Modeling of the Isotopic Effects During Snow Formation. J. Geophys. Res. 89: 11749-11757.

Jouzel J, Lorius C, Petit J R, Genthon C, Barkov N I, Kotlyakov V M, Petrov V M (1987) Vostok ice core: a continuous isotope temperature record over the last climatic cycle (160,000 years). Nature 329: 403-408.

Kraus E B (1972) Atmosphere-Ocean Interaction. Clarendon Press. Oxford. 275 p.

Lorius C, Raynaud D, Petit J-R, Jouzel J, Merlivat L (1984) Late-Glacial Maximum - Holocene atmospheric and ice-thickness changes from Antarctic ice-core studies. Annals of Glaciology 5: 88-94.

Lorius C, Jouzel J, Ritz C, Merlivat L, Barkov N I, Korotkevich Y S, Kotlyakov V M (1985) A 150.000-year climatic record from Antarctic Ice. Nature 316:591-596.

Mitchell A R, Griffiths D F (1980) The finite difference method in partial differential equations. John Wiley Chichester. 272pp.

Morland K W (1984) Thermomechanical balances of ice sheet flows. Geoph. Astroph. Fluid Mech. 29: 237-266.

Oerlemans J, Van der Veen C J (1984) Ice sheets and climate. Reidel. Dordrecht. 217 + xi p.

Paterson W S B, Budd W F (1982) Flow parameters for ice sheet modelling. Cold Regions Science and Technology 6:175-177.

Philberth K, Federer B (1971) On the temperature profile and age profile in the central part of cold ice sheets. J. Glaciology 10: 3-14

Ritz C (1987) Time dependent boundary conditions for calculation of temperature fields in ice sheets. IAHS Publ 170: 207-216

Robin G de Q (1955) Ice movement and temperature distribution in glaciers and ice sheets. J. Glaciology 2: 523-532

Robin G de Q (1983) (Ed.) The climatic record in polar ice sheets. Cambridge University Press. Cambridge. 212p.

Robin G de Q, Johnsen S J (1983) Atmospheric processes. in: Robin G de Q. (Ed) The climatic record in polar ice sheets. Cambridge University Press. Cambridge: 47-52.

Schubert G, Yuen D A (1982) Initation of ice ages by creep instability and surging of the East Antarctic ice sheet. Nature 296:127-130.

Weertman J (1968) Comparison between measured and theoretical temperature profiles of the Camp Century, Greenland, borehole. J.Geophys.Res. 73: 2691-2700.

Young N W (1981) Responses of ice sheets to environmental changes. IAHS Publ 131: 331-360

Yuen D , Saari M, Schubert G (1986) Explosive growth of shear-heating instabilities in the down-slope creep of ice sheets. J. Glaciology 32: 314-320.